Threshold characteristics of semiconductor microdisk lasers

R. E. Slusher, A. F. J. Levi, U. Mohideen, S. L. McCall, S. J. Pearton, and R. A. Logan
AT&T Bell Laboratories, Murray Hill, New Jersey 07974

(Received 18 March 1993; accepted for publication 28 June 1993)

This letter describes the threshold characteristics of InGaAs/InGaAsP microdisk lasers with optical emission near a wavelength $\lambda=1.52$ μm. More than 5% of the total spontaneous emission feeds into the lasing mode as the microdisk diameters reach 2 μm.

Whispering-gallery mode microdisk lasers using optical[1] and electrical[2] excitation have recently been demonstrated. The initial experiments[1] and results described here use continuous-wave optical excitation at liquid-nitrogen temperatures. The threshold characteristics of these microlasers are studied here as the small volume limit is approached where there is a single optical mode within the gain spectral region. We first develop a model for the microdisk modes and measure photoluminescent spectra which yield mode Q values and spacings. This model along with the measured threshold characteristics allows us to estimate the fraction β of the spontaneous emission that is emitted into the lasing mode. As this β parameter approaches its small volume limit of unity, the laser threshold pump powers are expected to decrease to very low values in the microwatt range and the nature of the threshold region is dramatically modified.

In a first approximation, a microdisk laser may be viewed as a semiconductor disk of thickness L suspended in vacuum. In a slab with $L\simeq\lambda/3n$, the lowest order transverse electric (TE) mode is dominant.[3] The vacuum wavelength is λ and $n(\omega)$ is the frequency dependent bulk refractive index of the semiconductor material. Two dimensional propagation of the lowest order TE mode is described by an effective refractive index $n_{\rm eff}$.[4]

Optical modes with trapped TE character within a dielectric disk may be approximated by solutions of the two-dimensional Helmholtz equation $(\nabla^2+n_{\rm eff}^2\omega^2/c^2)\psi=0$, where $\omega=2\pi c/\lambda$ and c is the speed of light in vacuum. Because of the cylindrical symmetry it is convenient to choose, for a given mode, $\psi=J_M(x)e^{iM\theta}$, where J_M are Bessel functions of the first kind, $x=n_{\rm eff}(\omega)\omega r/c$, and r, θ are polar coordinates. Radial mode numbers $N=1,2...$ are assigned where the corresponding mode frequencies, $\omega_{M,N}$ are in ascending order for fixed M. Cylindrical symmetry specifies $\omega_{M,N}=\omega_{-M,N}$ so that a twofold degeneracy exists for $M>0$. We abbreviate $\omega_{M,1}=\omega_M$. Boundary conditions are needed to determine the mode frequencies. Here we set $\psi=0$ at the disk radius R, so that $n_{\rm eff}(\omega)R\omega/c=x_M^{(1)}$, i.e., the smallest positive root of $J_M(x_M^{(1)})=0$. Microwave frequency measurements of similar modes in sapphire disks show that this is a good approximation.[5]

Quality factors[6] Q_m describing radiation loss from an ideal disk for the $N=1$ modes are expected, according to tunneling arguments,[1] to vary approximately exponentially, $Q_m=be^{2MJ}$, where $J=\tanh^{-1}(s)-s$, and $s=\sqrt{1-1/n_{\rm eff}^2}$. Comparison with exact results[7] for a dielectric sphere of refractive index $n_{\rm eff}$, for which identical tunneling arguments hold, leads to an estimate of the prefactor $b\sim 1/7$. In order to account for the relatively large dispersion[4] of $n_{\rm eff}$, the expression for Q_m should include an additional multiplicative factor $f_g=1+(\omega/n_{\rm eff})(dn_{\rm eff}/d\omega)$. Numerically f_g is near 1.51 assuming[8] $n(\omega)=[3.346+0.333(\hbar\omega-0.866\ {\rm eV})]$ for the materials and disk dimensions used in the experiments. The frequency dependence of $n_{\rm eff}$ also results in a factor of $1/f_g$ in the calculated mode spacing. Loss due to optical absorption in the cold cavity (pumping well below threshold) leads to $Q_a^{-1}=\alpha\lambda/2\pi n_{\rm eff}f_g$ where α is the absorption coefficient obtained by a suitable spatial average. The observed Q values should be compared with those determined by $Q^{-1}=Q_m^{-1}+Q_a^{-1}+Q_i^{-1}$, where Q_i^{-1} describes losses due to surface roughness, etc. The total radiation losses are characterized by Q_r where $Q_r^{-1}=Q_m^{-1}+Q_i^{-1}$. Q_r is typically limited by Q_i to values less than 1000. Q_a is a function of pump power and becomes a dominant limit to the Q value below threshold.

Two microdisks are studied experimentally, a "small" disk with $R=1.1$ μm, and a "large" disk with $R=2.5$ μm. Both disks have designed $L=0.15$ μm ($\simeq\lambda/3n$) and contain six 100 Å thick $In_{0.53}Ga_{0.47}As$ quantum wells separated by five 100 Å thick InGaAsP barriers and enclosed by two 200 Å thick InGaAsP barriers. The $n_{\rm eff}$ for this configuration[4,8] is 2.35. The composition of the InGaAsP barrier material has a room temperature band gap $E_g=1.1$ eV. The disk is supported by an InP pedestal of rhomboidal cross section.

Microdisk photoluminescence and lasing spectra are measured by illuminating with a $\lambda=0.6328$ μm HeNe laser that is focused to a waist $w_0=3.3(4.4)\mu$m for the small (large) disk. Typical spectra for the broad photoluminescence and narrow laser radiation are shown in Fig. 1. Cold cavity Q values, $\lambda_0/\Delta\lambda_0$, of 260(500) are measured for the small(large) disk from the photoluminescent spectrum at low pump powers below threshold in the range where the dominant cavity resonance line [seen in Fig. 1 at $\lambda_0=1505(1553)$ nm for the small (large) disk] has a full width half-maximum value $\Delta\lambda_0$.

At excitation levels well above threshold a second, shorter wavelength cavity mode appears in a few of the measured disks. As shown in the inset in Fig. 1, the measured mode spacing is 87 nm for the small disk and 37 nm for the large disk. Solutions to $n_{\rm eff}(\omega)\omega R/c=x_M^{(1)}$ for $M=1,2,...$ and $N=1$ determine the dominant high Q mode frequencies ω_M. Calculations of these mode wavelengths in the spectral region near 1500 nm yield $\lambda(M=7)=1482$ nm and $\lambda(M=6)=1593$ nm for the small disk and $\lambda(M=19)=1516$ nm and $\lambda(M=18)=1562$ nm for the large

 0003-6951/93/63(10)/1310/3/$6.00

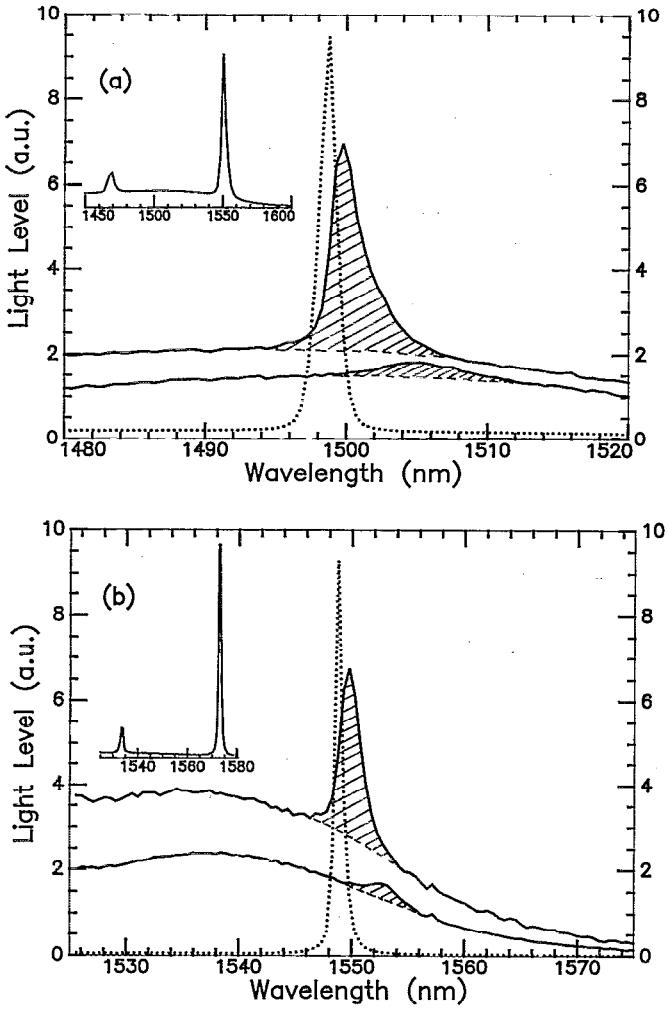

FIG. 1. Photoluminescence spectra of (a) a 2.2 μm diam microdisk and (b) a 5 μm diam microdisk mounted on a substrate cooled to liquid nitrogen temperatures. Excitation is by $\lambda=6328$ nm HeNe radiation at total absorbed power levels corresponding to below threshold (pump power, $P=10.6$ μW), at threshold ($P=24$ μW) and well above threshold ($P=76.2$ μW) (see Fig. 2). The corresponding powers in (b) are 19, 38, and 178 μW. The dotted curves for the data taken well above threshold are scaled by a factor of 12 and 92 for (a) and (b), respectively. The inserts show typical mode spacings for a 2.2 μm diameter microdisk (87 nm) and a 5 μm diam microdisk (37 nm) in (a) and (b), respectively. The shorter wavelength mode shown in the insert is only seen at very high pump powers where the spectrum is strongly broadened. The spectrometer resolution is 1 nm.

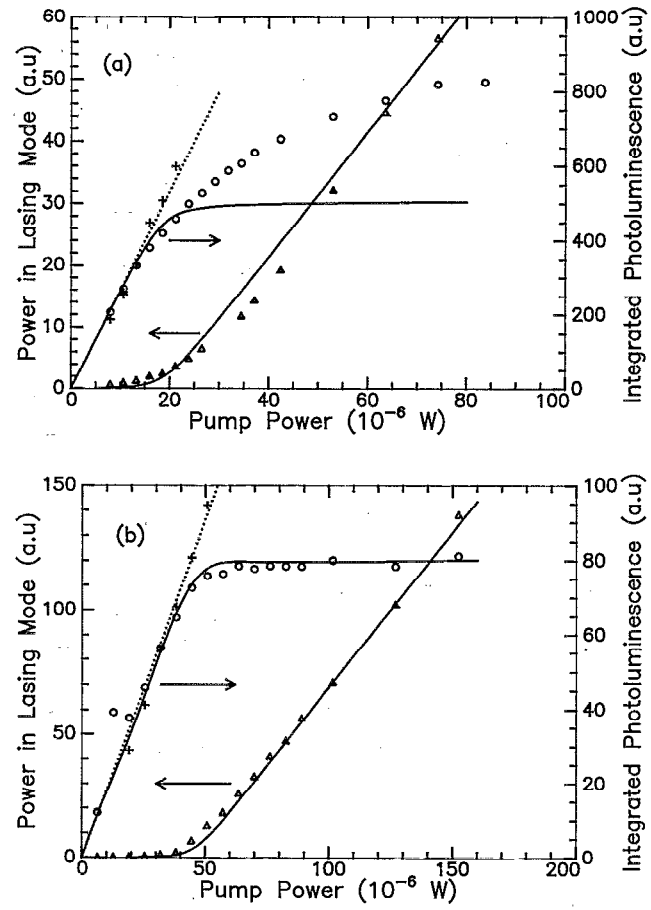

FIG. 2. The laser light output (triangles) and the spectrally integrated photoluminescence (circles) are shown as a function of pump power for a (a) 2.2 μm diam and (b) a 5 μm diam microdisk laser. The solid lines show rate equation simulations of the data. The rate equation parameters corresponding to (a) are $\beta\simeq0.23$ and $Q_r=500$ and in (b) are $\beta\simeq0.04$ and $Q_r=800$. The pump power plotted here is the absorbed power integrated over the entire disk area.

disk. A $M=7(19)$ yields a λ value closest to the laser mode frequency of the small(large) disk. The calculated mode spacings are in reasonable agreement with experiment.

The characteristics of the light output from the lasing mode and the spectrally integrated photoluminescence as a function of pump power absorbed in the disk are shown for the small and large microdisks in Figs. 2(a) and 2(b), respectively. The absorbed power is 0.6 times the incident power assuming 30% is lost by reflection and 85% of the remaining pump is absorbed. We define the laser line output to be the integrated light in the shaded region of the spectra shown in Fig. 1. The threshold of the small(large) microdisk obtained by an extrapolation from the linear lasing region is 25(45) μW. Carrier density pinning due to the dominance of stimulated emission above threshold is apparent from the leveling off of the photoluminescence near threshold. This pinning behavior is to be compared with the photoluminescence from nonlasing structures similar to the microdisks where a linear increase with pump power is observed over the entire pumping range as shown by the dashed lines and crossed data points in Fig. 2.

The fraction of the spontaneous emission that is emitted into the $M=7$, $N=1$ lasing mode of the small disk may be estimated by mode counting. We count the roots $x_M^{(i)}<x_7^{(1)}$ for each $M=0,1,...7$, multiply by the degeneracy $2(M>0)$ or $1(M=0)$ and sum to obtain 27 modes with eigenfrequencies less than or equal to ω_7. Since the density of states is linear with frequency, the state density at the lasing frequency is $27(2/\omega)$. The measured fractional bandwidth of the photoluminescence at pump powers well below threshold is $\delta\omega/\omega\simeq0.03$. This leads to an estimate of the fraction of the total spontaneous emission into the lasing mode at low pump powers, $\beta=(f_g 54\delta\omega/\omega)^{-1}\simeq0.41$. A small fraction of the spontaneous emission goes into free modes outside the disk and another small fraction is emitted into the TM1 mode,[3] finally reducing the β es-

timate by 0.7 to a value of 0.29. The β value is expected to scale with disk area so that $\beta=0.06$ is predicted for the large disk. We now demonstrate two methods for determining β from the experimental data and compare the results with our mode counting estimate.

The most direct measure of β is obtained from the relative levels of the spectrally integrated photoluminescence and the laser line output. At liquid nitrogen temperatures, the total quantum efficiency for emission from the InGaAs active material should be close to 100%. It follows that the total measured light output should vary linearly with pump power. This linearity is observed experimentally for the small microdisk using a value of 6 for the ratio of the luminescence to the laser line collection efficiency. Using this ratio we measure the fraction F of the total light emitted into the laser mode of the small microdisk to vary uniformly from 0.04 to 0.6 for pump powers from 5 to 80 μW. At transparency, where there is no net absorption of light emitted into the lasing mode, F corresponds to the definition of β. Transparency occurs just below threshold, in the pump power range between 10 and 25 μW where F is measured to vary from 0.05 to 0.18. Our best estimate of transparency corresponds to $F=\beta=0.15$. Below transparency, absorption at the laser mode frequency decreases F by a factor of $(1+Q_r/Q_a)^{-1}$.

A second, less direct, measure of β can be obtained by comparing the light output as a function of pump power in Fig. 2 with rate equation simulations. At liquid nitrogen temperatures the carrier loss rate can be assumed to be entirely due to spontaneous and stimulated emission. We simulate[9] spontaneous emission and gain using a three-dimensional density of states and quasi-Fermi levels for the electron and hole distributions. β, Q_r, and an effective radiative lifetime τ_r are used as fitting parameters for the data in Fig. 2. Electron and hole effective masses are taken to be $0.042m_e$ and $0.42m_e$, respectively, where m_e is the free electron mass. The entire volume of the disk shaped quantum wells are assumed to contribute to emission into the lasing mode. A Lorentzian width of 10 meV is used to characterize effects of carrier scattering on the emission process. The rate equation simulation fits to the data are shown as solid lines in Fig. 2. The fitting parameters for the small disk are $Q_r=500$ and $\tau_r=0.6$ ns. The β values are taken to vary inversely as the measured spontaneous emission linewidth. For the small disk the β values used to fit the data vary from 0.23 at low pump powers to 0.1 at the maximum pump power. For the large disk, the solid curves in Fig. 2(b) correspond to β between 0.06 and 0.04, $Q_r=800$ and $\tau_r=0.9$ ns. The rate equation predictions also agree with the observed flattening of the integrated spontaneous emission caused by carrier pinning. The increase in the integrated spontaneous emission above that predicted by the rate equation simulation seen in Fig. 2(a) can be accounted for with the observed emission from unpinned carriers in higher energy states.

In summary, the microdisk structures provide high Q whispering-gallery modes for disk radii small enough to restrict the estimated number of cavity modes with frequencies in the photoluminescent spectrum to less than five. This corresponds to estimated β values as large as 0.3. The measured β values range from 0.05 to 0.23 and depend on the pump level. The determination of β from the rate equations is not considered to be reliable to better than a factor of two. A number of factors are omitted from our rate equation analysis including a detailed treatment of carrier diffusion in the disk. We have assumed a single laser mode in the present analysis but there may be two nearly degenerate high Q modes at the laser line frequency. If both of these modes lased, the data should be compared with twice the mode counting estimate of β given above. A more complete analysis of the high β limit should use multimode rate equations. The data for the threshold characteristics and the mode counting estimates do show that the microdisk structures show promise for very low threshold, high β microlasers.

[1] S. L. McCall, A. F. J. Levi, R. E. Slusher, S. J. Pearton, and R. A. Logan, Appl. Phys. Lett. **60**, 289 (1992).

[2] A. F. J. Levi, R. E. Slusher, S. L. McCall, T. Tanbun-Ek, D. L. Coblentz, and S. J. Pearton, Electron. Lett. **28**, 1010 (1992).

[3] S. T. Ho, R. E. Slusher, and S. L. McCall, Quantum Electron Laser Sci. Technol. Dig. **11**, 54 (1991).

[4] H. C. Casey and M. B. Panish, *Heterostructure Lasers* (Academic, London, 1978), part A, p. 40.

[5] S. L. McCall, B. Yurke, L. D. Lanzarotti, and A. Pargellis (unpublished).

[6] The quality factor Q is defined by the temporal decay of the stored energy U where $U=\exp(-\omega_0 t/Q)$, where ω_0 is the angular resonant frequency of the mode.

[7] C. G. B. Garrett, W. Kaiser, and W. L. Bond, Phys. Rev. **124**, 1807 (1961).

[8] This is an estimate of the composite refractive index of the barriers and wells in the disk using frequency dependent indices from *Properties of Indium Phosphide*, EMIS data reviews series No. 6, Inspec, London, 1991.

[9] S. L. Chang, J. O'Gorman, and A. F. J. Levi, Special Issue IEEE J. Quantum Electron. Semicond. Lasers **29**, No. 6 (1993).